On Exotic Solutions of the Atmospheric Neutrino Problem.

Paolo Lipari and Maurizio Lusignoli

Dipartimento di Fisica, Università di Roma "la Sapienza",
and I.N.F.N., Sezione di Roma, P. A. Moro 2,
I-00185 Roma, Italy

Abstract

The measurements of the fluxes of atmospheric neutrinos give evidence for the disappearance of muon neutrinos. The determination of the dependence of the disappearance probability on the neutrino energy and trajectory allows in principle to establish unambiguosly the existence of neutrino oscillations. Alternative mechanisms for the disappearance of the neutrinos have been proposed, but do not provide a viable description of the data, if one includes both events where the neutrinos interact in the detector and ν–induced upward going muons. The proposed mechanisms differ in the energy dependence of the disappearance probability and the upward going muon data that are produced by high energy neutrinos give a crucial constraint.

1 Introduction

The measurements of the fluxes of atmospheric neutrinos by the Super–Kamiokande (SK) experiment [1, 2, 3, 4, 5] show evidence for the disappearance of muon (anti)–neutrinos. The same indication comes from the older data of the Kamiokande [6] and IMB [7] experiments and the recent ones of Soudan–2 [8]. Also the results recently presented by the MACRO collaboration [9, 10] indicate a suppression of the muon (anti)–neutrino flux.

The simplest explanation of the data is the existence of $\nu_\mu \leftrightarrow \nu_\tau$ oscillations [1]. In the framework of flavor oscillations one should consider the more general case of three flavors [11] (with the Chooz experiment [12] giving important contraints to the electron neutrino transitions), and could also envisage more complex scenarios involving sterile states [13]. We will not pursue these possibilities here, and we will adopt instead the simplest scenario of two–flavors oscillations as a prototype model that, as we will see, is able to describe successfully the experimental data.

We will instead investigate if other forms of 'new physics' beyond the standard model, different from standard flavor oscillations, can also provide a satisfactory description of

1

the existing data. Indeed several other physical mechanisms have been proposed in the literature as viable explanations of the atmospheric neutrino data. In this work we will consider three of these models: neutrino decay [14], flavor changing neutral currents (FCNC) [15, 16], and violations of the equivalence principle [17, 18] or, equivalently, of Lorentz invariance [19]. All these model have the common feature of 'disappearing' muon neutrinos, however the probability depends in different ways on the neutrino energy and path. To discriminate between these models a detailed study of the disappearance probability P and of its functional form is needed.

In this work in contrast with previous analyses we will argue that the present data allow to exclude the three 'exotic' models, at least in their simplest form, as explanations of the atmospheric neutrino problem. This is mainly due to the difficulty that these models have to fit at the same time the SK data for leptons generated inside the detector (sub– and multi–GeV) and for up–going muons generated in the rock below it.

2 Data

In fig. 1, 2 and 3 we show (as data points with statistical error bars) the ratios between the SK data and their Montecarlo predictions calculated in the absence of oscillations or other form of 'new physics' beyond the standard model. In fig. 1 we show the data for the e–like contained events, in fig. 2 for μ–like events produced in the detector, and in fig. 3 for upward-going muon events, as a function of zenith angle of the detected lepton. In each figure we include four lines: the dotted line (a constant of level unity) corresponds to exact agreement between data and no–oscillation Montecarlo, including the absolute normalization. The dot–dashed lines correspond to the assumption that there is no deformation in the shape of the zenith angle distributions, but that one is allowed to change the normalization of each data sample independently. The values obtained are: 1.16 for e–like sub-GeV, 1.21 for e–like multi-GeV, 0.72 for μ–like sub-GeV, 0.74 for μ–like multi-GeV, 0.56 for stopping upward-going muons, and 0.92 for passing upward-going muons. For two sets of data (sub-GeV and multi-GeV μ–like events) the constant shape fits give very poor descriptions ($\chi^2 = 26$ for the sub-GeV and 33 for the multi-GeV for 4 d.o.f). Also the zenith angle shape of the passing upward-going muons is not well fitted by the no–oscillation Montecarlo ($\chi^2 = 17$ for 9 degrees of freedom). The electron data do not show clear evidence of deformations, although the constant shape fit for the sub-GeV events ($\chi^2 = 9.7$ for 4 d.o.f.) is rather poor.

The normalizations of the different data sets are of course strongly correlated, and therefore it is not reasonable to let them vary independently. The other extreme option, that we will adopt in this work for simplicity, is to use one and the same parameter to fix the normalization of the six data samples. The result for constant shapes (i.e. assuming no 'new physics' beyond the standard model) is represented by the dashed lines in fig. 1, 2 and 3 corresponding to a value 0.84 and a very poor $\chi^2 = 280$ for 34 d.o.f.).

The full lines in the figures correspond to our best fit assuming $\nu_\mu \leftrightarrow \nu_\tau$ oscillations

2

with maximal mixing. We define the χ^2 as follows:

$$\chi^2 = \sum_j \left[\frac{N_j - \alpha\ N_j^{th}\ (N_{j,MC}^{SK}/N_{j,0}^{th})}{\sigma_j} \right]^2 \tag{1}$$

In (1) the summation runs over all data bins, N_j is the SK result for the j–th bin, σ_j its statistical error, N_j^{th} our prediction, $N_{j,0}^{th}$ our prediction in the absence of oscillations, $N_{j,MC}^{SK}$ the no–oscillation prediction of Super–Kamiokande, and α allows for variations in the absolute normalization of the prediction. We have rescaled our prediction to the SK Montecarlo because we do not have a sufficiently detailed knowledge of the detector response (e.g. number of detected rings) and efficiency. For the same same input neutrino spectra the difference between our no–oscillation calculation (see [20] for a description) and the SK Montecarlo result is approximately 10%,

For our best fit the values of the relevant parameters are $\alpha = 1.15$ and $\Delta m^2 = 3.2\ 10^{-3}$ eV^2. The χ^2 is 33.3 for 33 d.o.f.

Our definition of the χ^2 is somewhat simplistic. We do not take into account the contribution of systematic errors, either in the data or in the theory. The assumption of a common α for e–like and μ-like events corresponding to different energy regions is certainly too strict. It is therefore remarkable that this fit is so good, and essentially in agreement (same normalization and very near Δm^2 value) with the much more elaborate fit in [1].

In the rest of this paper we will consider other, 'exotic' models and we will find that they are not able to provide a satisfactory fit to the same data.

3 Models

We briefly recall the essential points of the models we are discussing.

For the usual, two–neutrino flavor oscillations the 'disappearance probability' P is given by:

$$P = P_{\nu_\mu \to \nu_\tau}^{osc} = \sin^2 2\theta\ \sin^2 \left[\frac{\Delta m^2}{4} \frac{L}{E_\nu} \right], \tag{2}$$

with the very characteristic sinusoidal dependence on the ratio L/E_ν.

In the simplest realization of neutrino decay, neglecting the possibility of the simultaneous existence of neutrino oscillations, the disappearance probability is given by:

$$P = P^{dec} = 1 - \exp \left[-\frac{m_\nu}{\tau_\nu} \frac{L}{E_\nu} \right], \tag{3}$$

still depending on the ratio between neutrino pathlength and energy L/E_ν, but with a functional form different from (2).

If flavor changing neutral currents contribute to the interaction of neutrinos with ordinary matter, a non trivial flavor evolution will develop even for massless neutrinos as

originally noted by Wolfenstein [21]. There are several theoretical models generically predicting nondiagonal neutrino interactions with matter. In particular such models have been proposed as a possible consequence of R-parity violating interactions in supersymmetric models and suggested as solutions of both the solar [22, 15] and atmospheric [15, 16] neutrino problems. Let us call $V_{\alpha\beta}$ the effective potential that arises from the forward scattering amplitude of a neutrino with a fermion f: $\nu_\alpha + f \to \nu_\beta + f$. In the standard model $V_{\mu\tau} = V_{\tau\mu} = 0$, and $V_{\mu\mu} = V_{\tau\tau} = \sqrt{2}\,G_F\,T_3(f_L)\,N_f$ where G_F is the Fermi constant, N_f is the number density of the fermion f and $T_3(f_L)$ is the third component of the fermion's weak isospin. Since the effective potentials for muon and tau neutrinos are identical, there is no effect on standard oscillations. However, if the scattering amplitudes are different from those predicted by the standard model, and if flavor changing scattering can occur, then the effective potential acquires non diagonal terms $V_{\mu\tau} = V_{\tau\mu} = \sqrt{2}G_F\epsilon N_f$, and different diagonal elements (with $V_{\tau\tau} - V_{\mu\mu} = \sqrt{2}G_F\epsilon' N_f$), and there will be a nontrivial flavor transition probability even for massless neutrinos. After the crossing of a layer of matter with a column density

$$X_f = \int_0^L dL' \; N_f(L') \,, \tag{4}$$

the transition probability is:

$$P = P_{\nu_\mu \to \nu_\tau}^{FCNC} = \frac{4\epsilon^2}{4\epsilon^2 + \epsilon'^2} \;\; \sin^2\left[\frac{G_F}{\sqrt{2}} X_f \sqrt{4\epsilon^2 + \epsilon'^2}\right]. \tag{5}$$

The probability has again an oscillatory form, however in this case the role of L/E_ν is taken by the column density X_f and there is no dependence on the neutrino energy.

If the gravitational coupling of neutrinos are flavor dependent (implying a violation of the equivalence principle) mixing will take place for neutrinos traveling in a gravitational field even for massless neutrinos [17, 18]. The neutrino states with well defined coupling to the gravitational field define a 'gravitational basis' related to the flavor basis by a unitary transformation. The effective interaction energy matrix of neutrinos in a gravitational field can be written in an arbitrary basis as

$$H = -2\,|\phi(r)|\; E_\nu(1+f) \tag{6}$$

where E_ν is the neutrino energy, $\phi(r) = -|\phi(r)|$ is the gravitational potential, and f is a (small, traceless) matrix that parametrize the possibility of non–standard coupling of neutrinos to gravity and is diagonal in the gravitational basis.

Much in the same way as in the previous cases, the noncoincidence of gravitational and flavor eigenstates determines mixing and flavor transitions. Considering the simple case of two flavors and assuming a constant gravitational potential $|\phi|$, the transition probability takes the form

$$P = P_{\nu_\mu \to \nu_\tau}^{grav} = \sin^2(2\theta_G)\; \sin^2[\delta|\phi|\,E_\nu\,L]. \tag{7}$$

where θ_G is the mixing angle and δ is the difference between the coupling to gravity of the gravitational eigenstates. Note that in this case the argument of the oscillatory function

is proportional to the product of the neutrino energy and pathlength, whereas for the standard flavor oscillations it is the ratio of the same quantities that matters.

Equations (2), (3), (5) and (7) are the disappearance probabilities for the four mechanisms that we will confront with the experimental data.

4 Flavor Oscillations

It is interesting to discuss how the usual flavor oscillations can successfully reproduce the pattern of suppression measured for the different event samples. The events detected in one particular bin are produced by neutrinos with a predictable distribution of E_ν and pathlength L, and therefore of L/E_ν, the significant quantity in flavor oscillations. In fig. 4, in the top panel we show as a function of L/E_ν the survival probability corresponding to maximal mixing and $\Delta m^2 = 3.2 \times 10^{-3}$ eV^2 (our best fit point). Also shown with a dashed line is the survival probability for neutrino decay that we will discuss in the next section.

In the second panel we show the L/E_ν distributions of sub–GeV μ–like events in the five zenith angle bins used by the SK collaboration: $\cos\theta_\mu \in [-1, -0.6]$, $[-0.6, -0.2]$ $[-0.2, +0.2]$, $[0.2, 0.6]$ and $[0.6, 1.0]$ (corresponding to the thick solid, thick dashed, thin dot–dashed, thin dashed and thin solid line).

In the third panel we show the corresponding distributions for multi-GeV μ–like events (same coding for the lines).

In the fourth panel we show the L/E_ν distributions for upward going muons that stop in the detector in the zenith angle bins: $\cos\theta_\mu \in [-1, -0.8]$, $[-0.8, -0.6]$ $[-0.6, -0.4]$, $[-0.4, -0.2]$ and $[-0.2, 0.0]$ with the corresponding lines ordered from right (higher values of L/E_ν) to left (lower values of L/E_ν).

In the last panel we show the same distributions for passing upward going muons in ten zenith angle bins, $\cos\theta_\mu \in [-1, -0.9], \ldots, [-0.1, 0.0]$.

Some remarks can be useful for an understanding of the distributions shown in fig. 4. For the sub-GeV events, one can see that the parent neutrinos have L/E_ν spread over a broad range of values. This is due to the poor correlation between the neutrino and muon directions $\langle\theta_{\nu\mu}\rangle \simeq 53°$.

For multi-GeV data the distributions are much narrower, reflecting the tighter correlation between the neutrino and muon directions, $\langle\theta_{\nu\mu}\rangle \simeq 13°$. Note also that the peaks in the L/E_ν distributions corresponding to sub-GeV and multi-GeV events in the same zenith angle interval are at slightly different points because of the different energy of the parent neutrinos.

For up–going stopping muons the width of the distribution is wider than in the multi-GeV case. The correlation between the muon and neutrino directions $\langle\theta_{\nu\mu}\rangle \simeq 10°$ is actually better, but the width of the distribution reflects the wider energy range of the neutrinos contributing to this signal. Passing muons are nearly collinear with the parent neutrinos ($\langle\theta_{\nu\mu}\rangle \simeq 2.9°$), but the large energy range of the neutrinos that extend over nearly two decades ($E_\nu \simeq 10–10^3$ GeV) results in a wide L/E_ν distribution.

All curves in the lower four panels of fig. 4 are normalized to unit area. In order to obtain the suppression due to oscillations in a particular bin, one has to perform the integral:

$$N_j^{osc}(\sin^2 2\theta, \Delta m^2) = \int dx \; \frac{dN_j^0}{dx} \; [1 - P^{osc}(x, \; \sin^2 2\theta, \Delta m^2)] \qquad (8)$$

Comparing the survival probability with the L/E_ν distributions it is easy to gain a qualitative understanding of the effects produced. For $\Delta m^2 \simeq 3 \cdot 10^{-3}$ eV^2, neutrinos with $L/E_\nu \lesssim 10^2$ Km/GeV have a survival probability close to unity and do not oscillate, while for neutrinos with $L/E_\nu \gtrsim 10^3$ Km/GeV, averaging over the rapid oscillations, the survival probability becomes one half for maximal mixing. We recall that horizontal neutrinos travel an average pathlength of $\simeq 600$ Km.

Taking into account the L/E_ν distributions of the different set of events one can see that all zenith angle bins of the muon sub–GeV events are somewhat suppressed, because even vertically downward going muons can be produced by upgoing neutrinos.

For multi–GeV events, with the tighter correlation between the neutrino and muon directions, the two up–going bins are suppressed by the 'average' factor ~ 0.5, the two down–going bins are left unchanged and the horizontal muons have an intermediate suppression.

The up–going stopping muons are always suppressed by a factor $\sim 1/2$, except for the bin nearest to the horizontal.

For the up–going passing muons the larger average energy and therefore smaller L/E_ν explains the smaller suppression and its pattern, varying from nearly unity for the horizontal bin to a maximum of ~ 0.65 for the vertical one.

5 Exotic Models

5.1 Neutrino Decay

Fitting the sub-GeV and multi-GeV data of Super-Kamiokande with the simplified model of muon neutrino decay (that neglects mixing) given in (3), we find a minimum in the χ^2 for a value $\tau_\nu/m_\nu = 8900$ Km/GeV (with $\alpha = 1.07$). This is in good agreement with the results of [14]. The authors of this reference have as a best fit point $\tau_\nu/m_\nu \simeq 12800$ Km/GeV, with a small mixing angle $\sin^2 2\theta \simeq 0.06$. The curve describing the decay probability for our best fit is shown as the dashed line in the top panel of fig. 4.

It is simple to have a qualitative understanding of the value of τ_ν/m_ν that provides the best fit. One needs to suppress by a factor ~ 0.5 the up-going multi-GeV muons that have $\langle L/E_\nu \rangle \simeq 10^{3.5}$ Km/GeV (see fig. 4).

The inclusion of decay results in $\chi^2 = 71$ (for 18 d.o.f.), a very significant improvement over the value 234 (19 d.o.f.) of the "standard model", but still significantly worse than the value $\chi^2 \simeq 25$ of the $\nu_\mu \leftrightarrow \nu_\tau$ flavor oscillation fit to the same set of data.

For a value of τ_ν/m_ν of the order of what is given by our fit to the sub–GeV and multi–GeV data, one expects a much smaller suppression of the high energy passing up–going muons (as already noted in [14]). In fact including also the 15 data points of the

up-going muons in a new fit, the best fit point becomes $\tau_\nu/m_\nu = 10000$ Km/GeV (similar to the previous one), but χ^2 increases to the much higher value 140.

5.2   Violation of the equivalence principle

Performing a fit to the sub-GeV and multi-GeV data of Super Kamiokande with the disappearance probability given by (7) and with maximal mixing ($\theta_G = \pi/4$), we find a minimum in the χ^2 for a value $\delta|\phi| = 4 \cdot 10^{-4}$ Km^{-1}GeV^{-1} (with $\alpha = 1.10$). The χ^2 for this fit is 35 for 18 d.o.f., still a very significant improvement over the standard model case, but not as good as the flavor oscillations result. The survival probability given by our best fit is shown in the top panel of fig. 5.

The reason of the poor χ^2 can qualitatively be understood looking at fig. 5. This figure is the equivalent of fig. 4, in the sense that the four lower panels show the distributions in the variable that is relevant in this case, namely $L \cdot E_\nu$. The distributions in this variable for the sub–GeV and multi–GeV events have shapes similar to the corresponding ones in L/E_ν, because the width of the distributions is mostly determined by the spread in pathlength L. However the average value of the $L \cdot E_\nu$ of the sub–GeV events is lower than the corresponding one (same zenith angle bin) for multi–GeV events, the opposite of what happens in the L/E_ν distributions, see fig. 4. Therefore, parameters describing well multi–GeV events will generally produce too low a suppression for sub–GeV events or viceversa.

It can be argued (as the authors of reference [24] do) that taking into account systematic uncertainties the model defined by equation (7) provides a good fit to the data, however this is not the case if upward–going muons are included in the picture. This should be evident looking at the lower panels in fig. 5. Upward–going muons are produced by high energy neutrinos and the frequent oscillations do imply a suppression by 50% of passing (and stopping) muons, with no deformation of the zenith angle distribution. This is in disagreement with the corresponding data: in fact, trying to fit all the data together we obtain similar best fit parameters, $\delta|\phi| = 4.5 \cdot 10^{-4}$ Km^{-1}GeV^{-1} and $\alpha = 1.145$, but with a very bad $\chi^2 = 142.7$ for 32 d.o.f. (the contribution of passing upward–going muon data being ~ 100).

5.3   Flavor Changing Neutral Currents

In the case of neutrino transitions produced by flavor changing neutral currents, the rôle of L/E_ν is replaced by X, the column density. This has the fundamental consequence that there is no energy dependence of the flavor conversion. Moreover since air has a density much lower that the Earth's, the transitions do not develop during the neutrino path in the atmosphere, and therefore down–going neutrinos are unaffected. Note also that there is not a simple relation between the zenith angle θ_ν and the pathlength L because of fluctuations in the neutrino birth position. However, due the air low density, the zenith angle θ_ν does define the column density X with a negligible error: the entire down–going hemisphere corresponds to $X \simeq 0$ and to a vanishing transition probability.

7

Performing, as before, a fit to the sub-GeV and multi-GeV data of Super Kamiokande with the disappearance probability given by (5) and assuming scattering off down quarks and $\epsilon' = 0$ (that is maximal mixing), we obtain a best fit value $\epsilon = 0.4$ and $\alpha = 1.08$ corresponding to a minimum $\chi^2 = 38$. With increasing ϵ the oscillations become more frequent, and essentially all values $\epsilon \gtrsim 0.4$ give comparable fits, since for these large values the oscillations can be considered as averaged in the entire up–going hemisphere.

The authors of reference [16], exploring the parameter space (ϵ, ϵ') find two solutions: (a): (0.98,0.02) and (b): (0.08,0.07), that are plotted in the upper panels of fig. 6. The first solution corresponds to the one that we have found, considering the slow variation of χ^2 with ϵ in the large ϵ region. The χ^2 found by the authors of [16] is however better that what we find, indeed as good as in the flavor oscillation model.

We do find that fitting the muon data only, without considering the constraint on the normalization coming from the electron data, the FCNC model gives an excellent fit, indeed as good or better than the flavor oscillation model. The reason why, in our fitting procedure, the FCNC model gives not as good a fit originates from the fact that the theoretical average value of the suppression for both sub–GeV and multi–GeV muon events for the best fit parameters is $\simeq 0.75$, corresponding to no suppression in the down–going hemisphere and ~ 0.5 in the opposite one. The data [2, 3] for the double ratio $R = (\mu/e)_{Data}/(\mu/e)_{MC}$: $R_{sub} = 0.61 \pm 0.03 \pm 0.05$, and $R_{multi} = 0.66 \pm 0.06 \pm 0.08$ indicate a larger average suppression. The allowance of a non perfect correlation between the normalizations of the muons and electron data samples would certainly reduce the χ^2 value of our fit.

The inclusion of up–going muons among the data considered, again results in evidence against this model. We recall the fact that the passing muons are essentially collinear with the parent neutrinos and that the experimental zenith angle distribution does not exhibit large sharp features as those predicted for example by solution (b) of [16] (see fig. 6). Therefore the relative smoothness of the passing muon data allows to exclude a large range of values (ϵ, ϵ') that correspond to few oscillations in the up–going hemisphere (that is $0.04 \lesssim \sqrt{4\epsilon^2 + \epsilon'^2} \lesssim 0.2$) and still large effective mixing $\epsilon \gtrsim \epsilon'$.

The solution (a) of [16] cannot be excluded using this consideration, because its frequent oscillations do not produce sharp features given the binning of the experimental data, and give a constant suppression $2\epsilon^2/(4\epsilon^2 + \epsilon'^2)$ for all zenith angle bins. The model has no energy dependence, and therefore this average suppression must apply to the up–going passing and stopping events, as well as to the up–going multi–GeV events, that have also a rather sharp correlation between the neutrino and muon directions. This is in disagreement with two features of the experimental data: (i) the passing muons have a suppression considerably less than both the stopping and up–going multi–GeV muons; (ii) the shape of the zenith angle distribution of passing muons shows evidence for a deformation. More quantitatively, a fit to all the data with $\epsilon' = 0$ gives the parameter values $\epsilon = 1.4$ and $\alpha = 1.12$ but with a total $\chi^2 = 149$ (the contribution to χ^2 of the throughgoing muon data being 105).

8

6   Summary and conclusions

The survival probability $P(\nu_\mu \to \nu_\mu)$ in the case of two flavor $\nu_\mu \leftrightarrow \nu_\tau$ oscillations has a well defined dependence on the pathlength and energy of the neutrinos. In order to establish unambiguosly the existence of such oscillations it is necessary to study in detail these dependences. In the analysis of the events interacting in the detector, one can study a very wide range of pathlengths ($10 \lesssim L \lesssim 10^4$ Km) but a much smaller range of neutrino energies close to 1 GeV (the sub–GeV and multi–GeV samples). Therefore it is not easy to obtain experimental information on the dependence of the survival probability on the neutrino energy. In fact models where the combination L/E_ν (flavor oscillations), $L \cdot E_\nu$ (violations of the equivalence principle) and $X \simeq L$ (flavor changing neutral currents) is the relevant variable for an oscillating transition probability, have been proposed as viable solutions of these data. Neutrino decay is also dependent on the ratio L/E_ν, but with a different functional form.

In this study we find that flavor oscillations provide a significantly better fit to the sub–GeV and multi–GeV data samples than the exotic alternatives we have considered, however with a generous allowance for systematic uncertainties the alternative explanations can still be considered as viable. Including the upward going muons in the fit the alternative models are essentially ruled out.

The upward–going muons are a set of ν–induced events corresponding to much larger E_ν: for passing muons the median parent neutrino energy is approximately 100 GeV, with a significant contribution of neutrinos with energy as large as 1 TeV, and therefore are in principle a powerful handle to study the energy dependence of the neutrino survival probability. If flavor oscillations (where L/E_ν is the significant variable) are the cause of the suppression of sub–GeV and multi–GeV muon events, the neutrinos producing passing upward going muons must also oscillate, but with a smaller suppression because of their larger energy; moreover, for the range of Δm^2 suggested by the lower energy data, one expects a moderate but detectable deformation of the zenith angle distribution. Both effects are detected.

In the alternative exotic models we have studied here, high energy events, such as the passing upward–going muons, are suppressed much more $(L \cdot E_\nu)$ than or as much $(X \sim L)$ as the up–going multi–GeV events, in contrast to the experimental evidence.

Also in the case of neutrino decay, the upward–going muon data are very poorly fitted by the model. Of course if neutrino have different masses (and can decay) it is natural to expect oscillations in combination with decay. We have not explored this possibility, but we can conclude that decay cannot be the dominant form of muon neutrino disappearance.

Two results of the measurements of upward going–muons are critically important to allow discrimination against exotic models and in favour of usual oscillations:

- the stopping/passing (Data/Montecarlo) double ratio for the SK upward–going muons [5] is $r = 0.56$, with a combined statistical and experimental systematic error of 0.07. The theoretical uncertainty in the relative normalization of the two sets of data has been estimated as 8% in [25]; more conservatively the SK collaboration [5] has used 13%. Quadratically combining the more conservative estimate

9

of the theoretical uncertainty with the experimental errors, the resulting σ_r is 0.1. Therefore the suppression for the high energy passing muons, is weaker than for the lower energy stopping ones at more than four sigma of significance, even allowing for a rather large uncertainty in the theoretical prediction. This is in contrast with models that predict for the stopping/passing double ratio r a value of unity (flavor changing neutral currents) or larger (violations of the equivalence principle).

- The shape of the through–going upward–going muons zenith angle distribution shows indication of a deformation, although the no–distortion hypothesis (with free normalization) has a probability close to 5%. The deformation if present is a rather smooth one, and the distribution can be used to rule out models (such as FCNC with smallish ϵ) that produce deep and marked features in the neutrino distribution (well mapped by the nearly collinear muons).

The MACRO collaboration has also obtained results on upward–going muons [9], that indicate the presence of an angular deformation compatible with the presence of flavor oscillations (although the oscillation fit even if significantly better that the standard model fit is still rather poor). Preliminary results on events where upward–going muons are produced in (and exit from) the detector, and a second class of events that combines stopping upward–going muons and downward–going muons produced in the detector indicate a pattern of suppression that is only compatible with an oscillation probability that decreases with energy [10].

Also the Kamiokande collaboration [26] has measured passing upward–going muons with results in good agreement with Super–Kamiokande, while the Baksan collaboration [27] has obtained results not in good agreement. One should also note that the IMB collaboration has in the past measured a stopping/passing ratio for upward–going muons in agreement with a no oscillation Montecarlo prediction [28] (see [29] for a critical analysis).

In conclusion, we find that the present data on atmospheric neutrinos allow to determine some qualitative features of the functional dependence of the disappearance probability for muon neutrinos. This probability (smeared by resolution effects) increases with the pathlength L producing the up/down asymmetry that is the strongest evidence for physics beyond the standard model. The difference in suppression between the sub(multi)–GeV muon events and the higher energy through–going muons indicates that the transition probability decreases with energy. These results are in agreement with the predictions of $\nu_\mu \leftrightarrow \nu_\tau$ oscillations and in contrast with several alternative exotic models. If flavor oscillations are indeed the mechanism for the muon neutrinos disappearance, additional data with more statistics and resolution (in L and E_ν) should allow to study in more detail the oscillatory structure of the transition probability as a function of the variable L/E_ν, unambiguosly determining the physical phenomenon. It is natural to expect that the oscillations involve all flavors and that electron neutrinos participate in the oscillations (with a reduced mixing because of the Chooz limit). The resulting flavor conversions will have a more complex dependence on the neutrino path and energy E_ν; the detection of these more subtle effects could become the next challenge for the experimentalists.

References

[1] Y. Fukuda et al (Super-Kamiokande collaboration), Phys.Rev.Lett. **81**, 1562 (1998) (also hep-ex/9807003).

[2] Y. Fukuda et al (Super-Kamiokande collaboration), Phys. Lett. B **433**, 9 (1998) (also hep-ex/9803006).

[3] Y. Fukuda et al (Super-Kamiokande collaboration), Phys. Lett. B **43**, 33 (1998) (also hep-ex/9805006).

[4] The Super-Kamiokande Collaboration, hep-ex/9812014, submitted to PRL (1998).

[5] Takaaki Kajita, for the Super-Kamiokande and Kamiokande collaborations, hep-ex/9810001, to appear in the proceedings of XVIII International Conference on Neutrino Physics and Astrophysics (Neutrino'98), Takayama, Japan, 4-9 June 1998.

[6] Kamiokande collaboration, K.S. Hirata et al, Phys. Lett. B **205**, 416 (1988), Phys. Lett. B **280**, 146 (1992);
Kamiokande collaboration, Y. Fukuda et al, Phys. Lett. B **335**, 237 (1994).

[7] IMB collaboration, D. Casper et al, Phys. Rev. Lett. **66**, 2561 (1991);
IMB collaboration, R. Becker-Szendy et al, Phys. Rev. D **46**, 3720 (1992).

[8] W.W.M. Allison et al, Phys. Lett. B **391**, 491 (1997);
T. Kafka for the Soudan–2 collaboration, Nucl.Phys.Proc.Suppl. **70**, 340, (1999).

[9] M. Ambrosio *et al.*, (MACRO collaboration) Phys. Lett. B **434**, 451 (1998) (also hep-ex/9807005).

[10] F. Ronga (for the MACRO collaboration), hep-ex/9810008, to appear in the proceedings of XVIII International Conference on Neutrino Physics and Astrophysics (Neutrino'98), Takayama, Japan, 4-9 June, 1998

[11] G.L. Fogli, E. Lisi, D. Montanino, and G. Scioscia, Phys. Rev. D **55**, 4385 (1997);
G. Fogli, E. Lisi, A. Marrone and G. Scioscia, hep-ph/9808205 (1998);
C. Giunti, C.W. Kim, M. Monteno, Nucl.Phys. B **521**, 3, (1998);
O. Yasuda, Phys.Rev. D **58**, 091301 (1998);
V. Barger, T.J. Weiler, and K. Whisnant, Phys.Lett. B **440**, 1 (1998).

[12] M. Apollonio et al, Phys. Lett. B **240**, 397 (1998).

[13] E. Akhmedov, P. Lipari and M. Lusignoli, Phys. Lett. b **300**, 128 (1993);
Q. Liu and A. Smirnov, Nucl. Phys. B **524**, 505 (1998);
R. Foot, R. Volkas and O. Yasuda, hep-ph/9801431 (1998);
Q. Liu, S. Mikheyev and A. Smirnov, Phys.Lett. B **440**,319 (1998);
P. Lipari and M. Lusignoli, Phys. Rev. D **58**, 073005 (1998);
M.C. Gonzalez-Garcia et al, hep-ph/9807305 (1998).

[14] V. Barger, J. G. Learned, S. Pakvasa and T. J. Weiler, astro-ph/9810121, submitted to PRL (1998).

[15] G. Brooijmans, hep-ph/9808498 (1998).

[16] M. C. Gonzalez-Garcia *et al.*, hep-ph/9809531 (1998).

[17] M. Gasperini, Phys. Rev. D **38**, 2635 (1988); Phys. Rev. D **39**, 3606 (1989).

[18] A. Halprin and C. N. Leung, Phys. Rev. Lett. **67**, 1833 (1991);
A. Halprin and C. N. Leung, Nucl. Phys. B (Proc. Suppl.) **28A**, 139 (1992);
J. Pantaleone, A. Halprin and C.N.Leung, Phys.Rev. D **47**, 4199 (1993);
A. Halprin, C. N. Leung and J. Pantaleone, Phys.Rev. D **53**, 5365 (1996).

[19] S. Coleman and S.L. Glashow, Phys.Lett. B **405**, 249 (1997);
S.L. Glashow, A. Halprin, P.I. Krastev, C.N. Leung and J. Pantaleone,
Phys.Rev. D **56**, 2433 (1997).

[20] E.Kh Akhmedov, A.Dighe, P.Lipari and A.Yu.Smirnov, hep-ph/9808270, to appear in Nucl.Phys.B (1999).

[21] L. Wolfenstein, Phys. Rev. D**17**, 2369 (1978); Phys. Rev. D **20**, 2634 (1979).

[22] M.M. Guzzo, A. Masiero and S.T. Petcov, Phys. Lett. B **260**, 154 (1991);
E. Roulet, Phys. Rev. D **44**, 935 (1991);
V. Barger, R.J.N. Phillips and K. Whisnant, Phys.Rev. D **44**, 1629 (1991);
P.I. Krastev and J.N. Bahcall, hep-ph/9703267 (1997).

[23] M. Mikheyev and A. Smirnov, Sov.J.Nucl.Phys. **42**, 913 (1986).

[24] R. Foot, C. N. Leung and O. Yasuda, hep-ph/9809458

[25] P. Lipari and M. Lusignoli, Phys.Rev. D **57**, 3842 (1998).

[26] Kamiokande Collaboration, S. Hatakeyama et al, Phys. Rev. Lett. **81**, 2016 (1998).

[27] Baksan Collaboration, M. M. Boliev et al, ICRC '95, Rome, Vol 1, p. 686; *ibidem*, p. 722.

[28] IMB collaboration, R. Becker-Szendy et al, Phys. Rev. Lett. **69**, 1010 (1992).

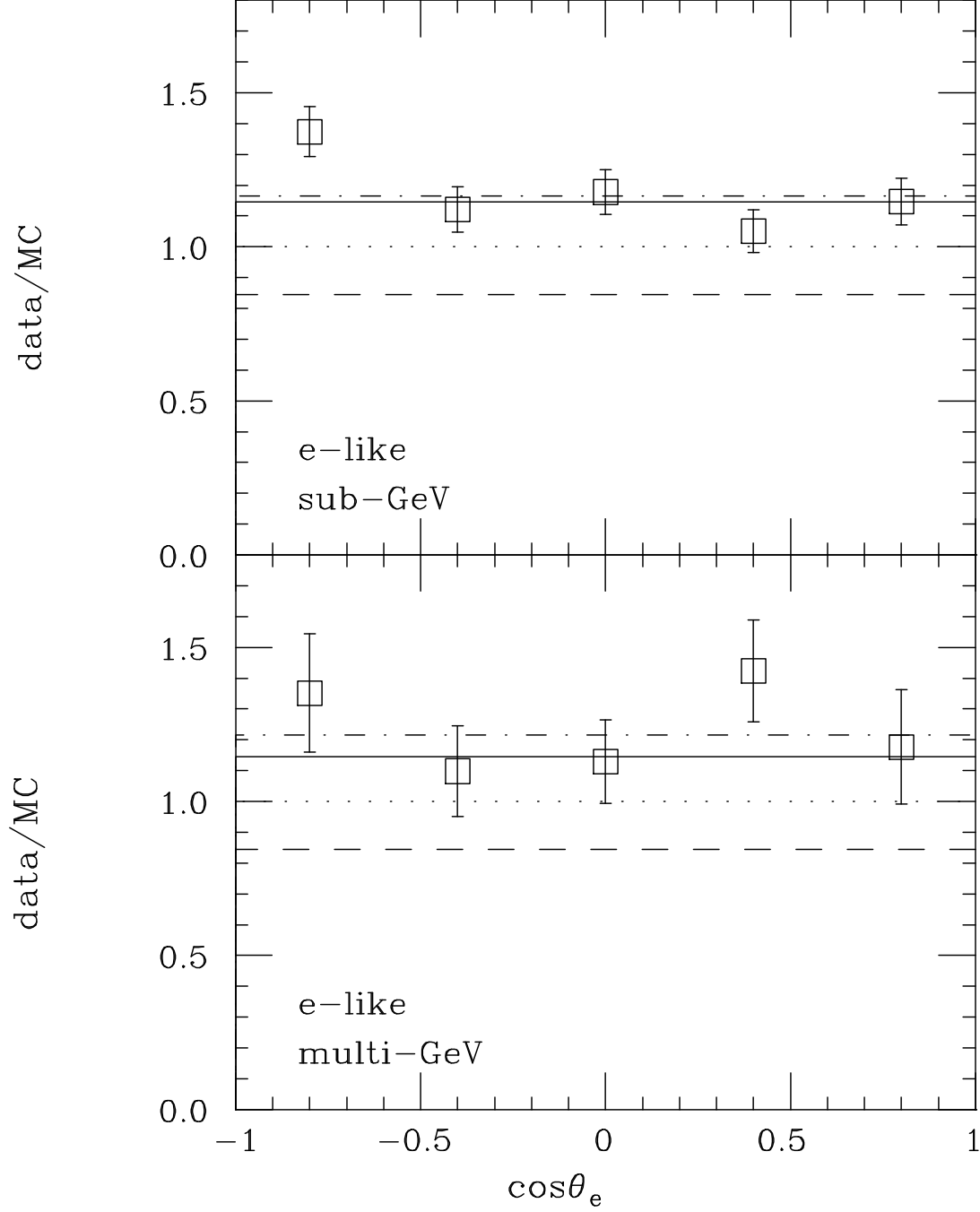[29] P. Lipari, M. Lusignoli, and F. Sartogo, Phys.Rev.Lett. **74**, 4384 (1995).

Figure 1: Ratio Data/Montecarlo for the e–like events of Super–Kamiokande. The dot–dashed lines are straight line fits (independent for each panel) to the data points; the dashed lines are the result of fitting all data (included in fig. 1, 2 and 3) with a common normalization ($\alpha = 0.84$); the solid lines are the result of a calculation with $\nu_\mu \leftrightarrow \nu_\tau$ oscillations with our best fit parameters for maximal mixing ($\Delta m^2 = 3.2 \times 10{-}3$ eV^2 and a normalization $\alpha = 1.15$).

13
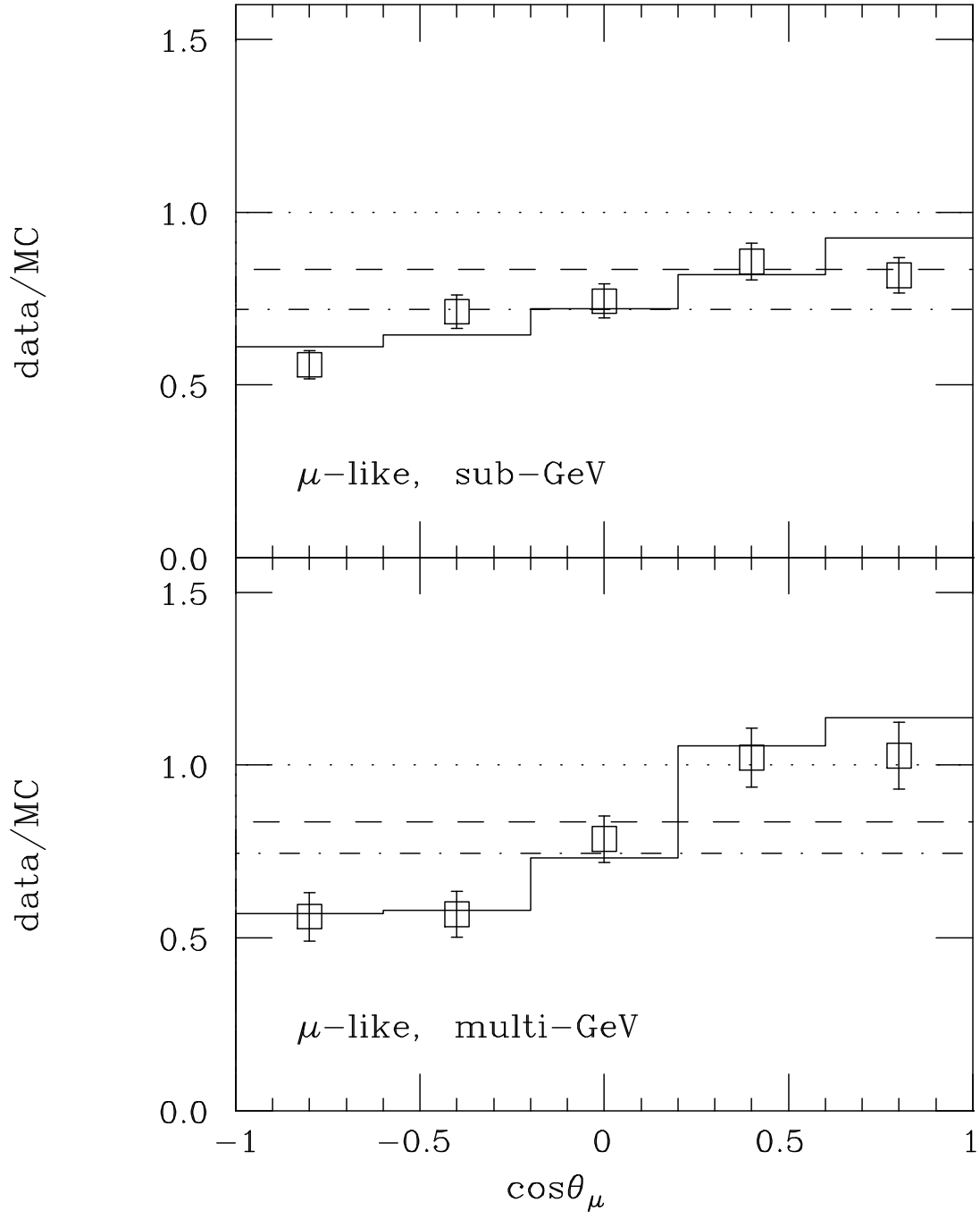
Figure 2: Ratio Data/Montecarlo for the μ–like events of Super–Kamiokande. See fig. 1 for a descrition of the lines.
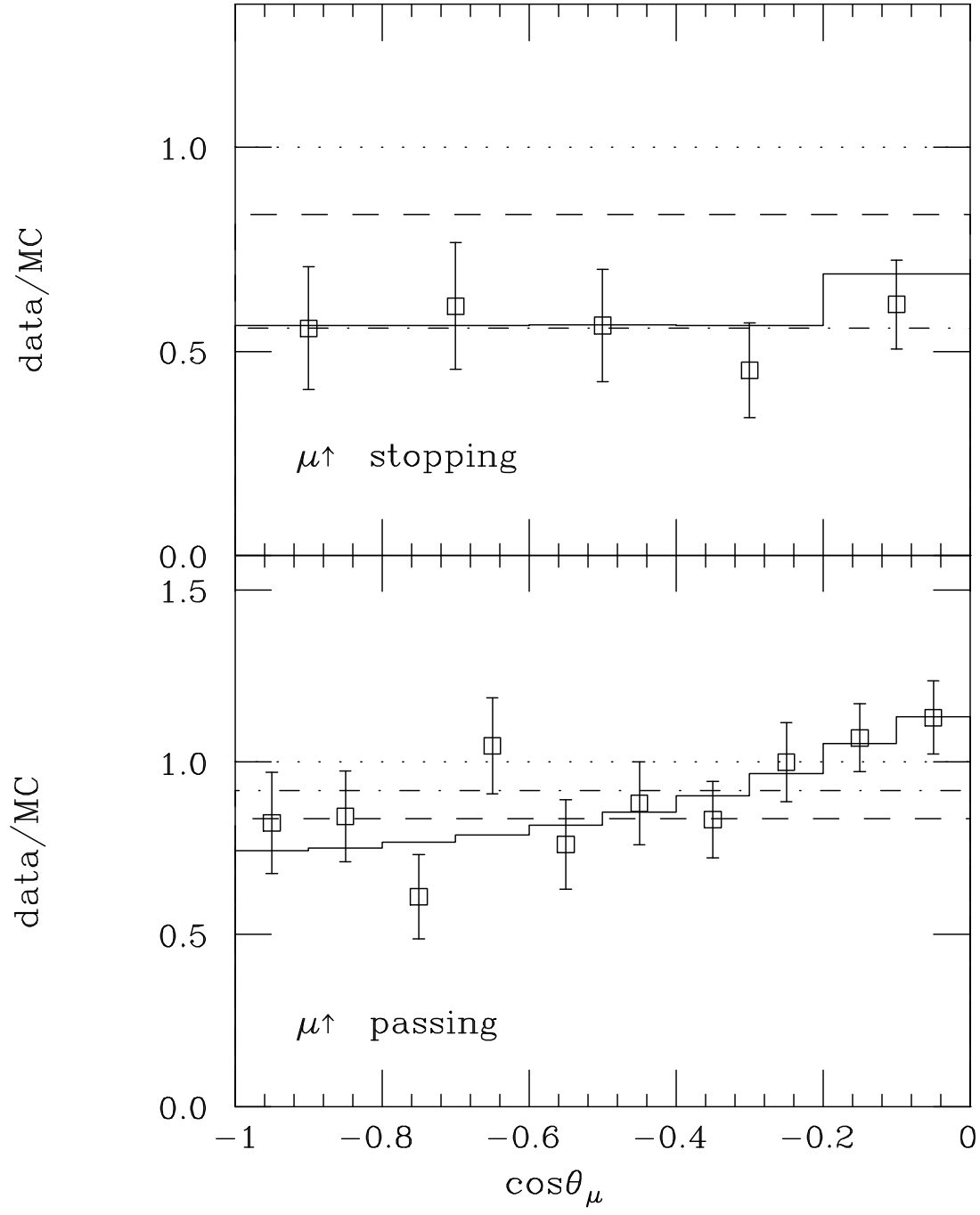
Figure 3: Ratio Data/Montecarlo for passing and stopping upward–going muons in Super–Kamiokande. See fig. 1 for a descrition of the lines.
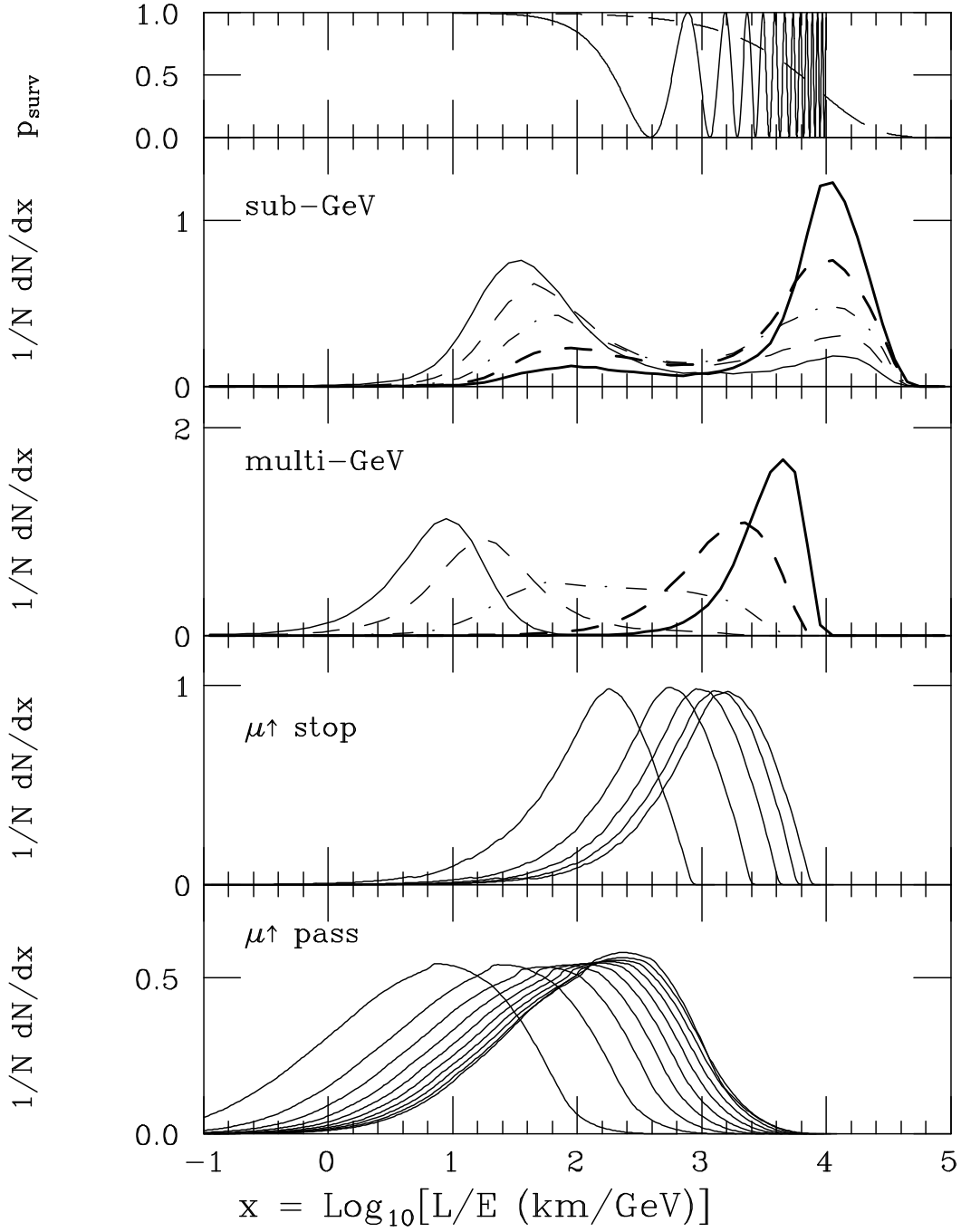
Figure 4: Distributions in L/E_ν for the different event classes considered. In the top panel we show the survival probability $P(\nu_\mu \to \nu_\mu)$ for our best fit with flavor oscillations to all data (solid line) and the best fit with neutrino decay to the sub–GeV and multi–GeV data (dashed line).
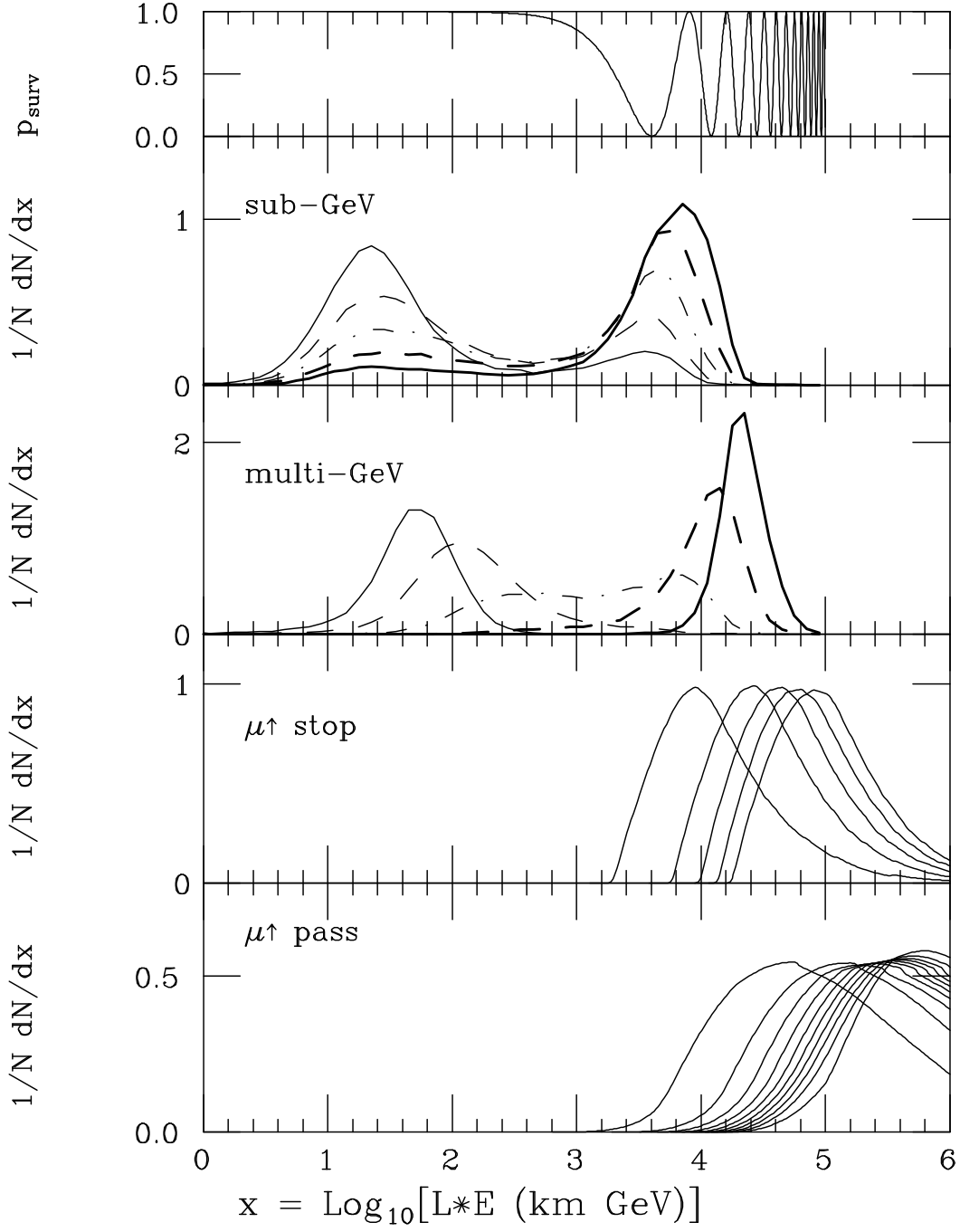
Figure 5: Distributions in $L \cdot E_\nu$ for the different event classes considered. In the top panel we show the survival probability $P(\nu_\mu \rightarrow \nu_\mu)$ for our best fit to the sub–GeV and multi–GeV data.
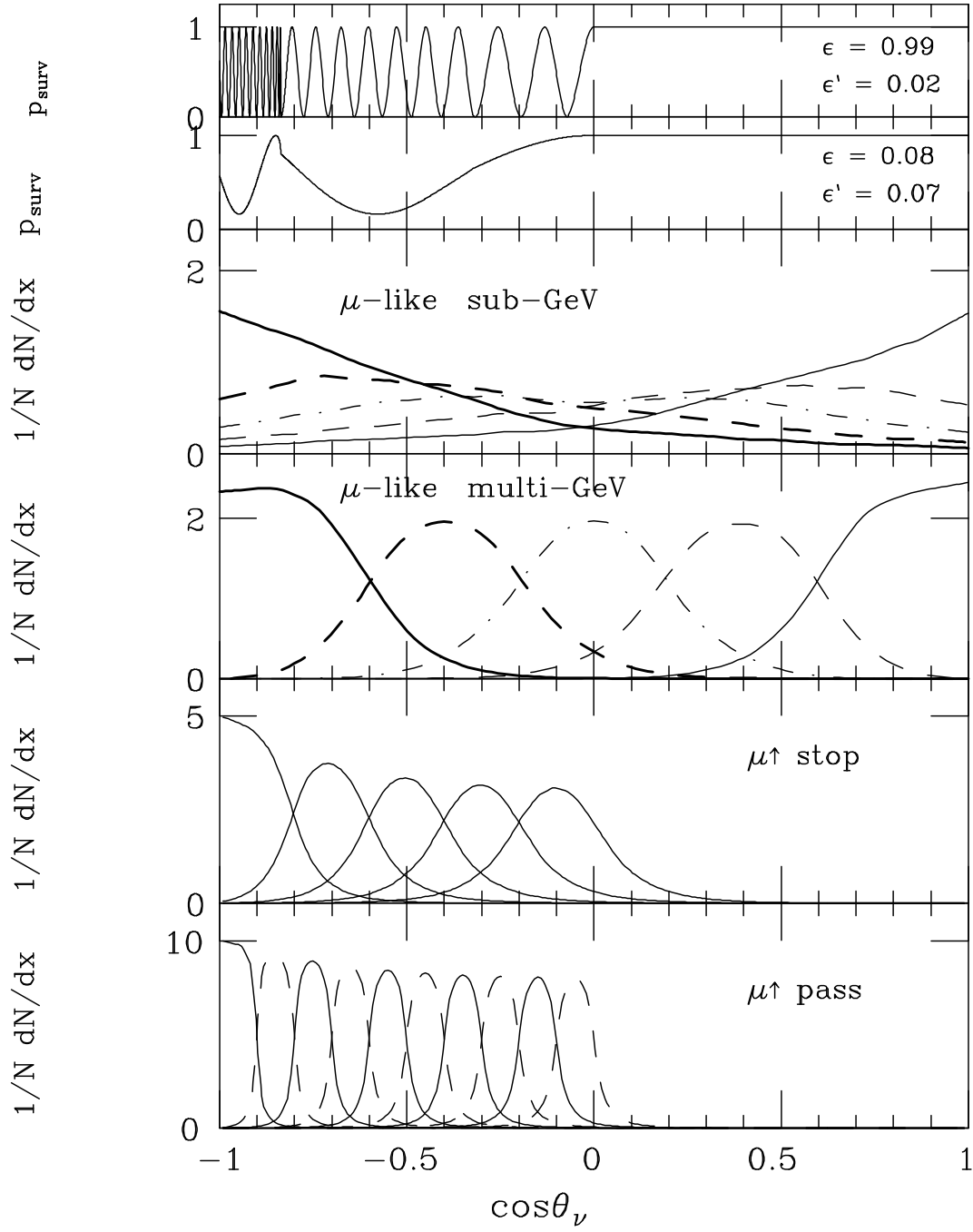
17

Figure 6: Distributions in $\cos\theta_\nu$ for the different event classes considered. In the two top panels we show the survival probability $P(\nu_\mu \to \nu_\mu)$ of the two best fit points as calculated in [16].